Macrophage insulin receptor deficiency increases ER stress-induced apoptosis and necrotic core formation in advanced atherosclerotic lesions

Seongah Han,[1,2,*] Chien-Ping Liang,[1,2,*] Tracie DeVries-Seimon,[1] Mollie Ranalletta,[1] Carrie L. Welch,[1] Kadesha Collins-Fletcher,[1] Domenico Accili,[1] Ira Tabas,[1] and Alan R. Tall[1]

[1] Departments of Medicine, Anatomy and Cell Biology, and Physiology and Cellular Biophysics, Columbia University, New York, New York 10032
[2] These authors contributed equally to this work.
*Correspondence: sh2068@columbia.edu (S.H.); cl534@columbia.edu (C.-P.L.)

Summary

Insulin resistance in diabetes and metabolic syndrome is thought to increase susceptibility to atherosclerotic cardiovascular disease, but the underlying mechanisms are poorly understood. To evaluate the possibility that decreased insulin signaling in macrophage foam cells might worsen atherosclerosis, *Ldlr*$^{-/-}$ mice were transplanted with insulin receptor *Insr*$^{+/+}$ or *Insr*$^{-/-}$ bone marrow. Western diet-fed *Insr*$^{-/-}$ recipients developed larger, more complex lesions with increased necrotic cores and increased numbers of apoptotic cells. *Insr*$^{-/-}$ macrophages showed diminished Akt phosphorylation and an augmented ER stress response, leading to induction of scavenger receptor A and increased apoptosis when challenged with cholesterol loading or nutrient deprivation. These studies suggest that defective insulin signaling and reduced Akt activity impair the ability of macrophages to deal with ER stress-induced apoptosis within atherosclerotic plaques.

Introduction

Atherosclerosis is a disease of arterial lipid deposition leading to a number of biological responses, including a chronic, macrophage-dominated inflammatory reaction (Hansson, 2005). Following the retention of LDL on the arterial matrix, and its modification by oxidation or aggregation, macrophages migrate into the arterial wall, take up the modified LDL, store its lipid as cholesterol and cholesterol esters and thus give rise to lipid-laden foam cells (Glass and Witztum, 2001; Hansson, 2005; Williams and Tabas, 1998). Foam cells have a central role both in the formation of early fatty streak lesions, as well as in the evolution of more complex atherosclerotic plaques. Death of foam cells by necrosis or apoptosis, particularly in the face of defective phagocytic clearance of the dead foam cells, is thought to give rise to large regions within plaques containing extracellular lipid and necrotic debris (Tabas, 2005). The fissuring or erosion of these complex plaques leads to thrombotic occlusion of coronary and cerebral vessels producing the clinical complications of atherosclerosis (Libby, 2002; Tabas, 2004).

Diabetes is a major risk factor for atherosclerotic cardiovascular disease, but the underlying mechanisms are poorly understood. There is only limited evidence that hyperglycemia promotes atherosclerosis in humans (Nathan et al., 2003), and in many experimental models, hyperglycemia does not induce atherogenesis independent of hyperlipidemia (Brownlee, 2001; Vikramadithyan et al., 2005). Insulin resistance is thought to give rise to many of the complications of metabolic syndrome and Type II diabetes, and in some studies hyperinsulinemia is an independent risk factor for atherosclerotic macrovascular disease (Pirro et al., 2002). Insulin resistance in classical insulin target organs such as liver, muscle, and adipose can lead to hyperinsulinemia, dyslipidemia, hypertension, and hypercoagulability, all factors that may predispose to atherosclerotic cardiovascular disease (Ginsberg, 2000; Reaven, 2002).

Recent studies have suggested that insulin resistance in cells of the arterial wall might also promote atherosclerosis. Insulin signaling in endothelium may be important in maintaining NO-mediated arterial responses. Diabetics have defective NO-dependent induction of arterial blood flow (Steinberg and Baron, 2002), and an endothelial-specific KO of the insulin receptor leads to decreased endothelial eNOS expression (Vicent et al., 2003). Our recent studies have suggested that defective macrophage insulin signaling predisposes to foam cell formation in atherosclerotic lesions. Macrophages from obese (ob/ob) mice were found to have reduced expression and signaling of insulin receptors (Liang et al., 2004), a posttranscriptional increase in scavenger receptor A (SRA) and CD36, and increased uptake of modified LDL particles. Similar changes were found in insulin receptor (Insr)-deficient macrophages (Liang et al., 2004). Thus, the increased expression of CD36 and SRA in macrophages with defective insulin signaling might be expected to increase foam cell formation and atherogenesis (Liang et al., 2004). However, recent studies have suggested a limited role of SRA and CD36 in the formation of early atherosclerotic lesions, perhaps related to redundant mechanisms for foam cell formation in vivo (Moore et al., 2005).

In order to evaluate the effect of macrophage insulin resistance on atherogenesis, we performed BM transplantation studies from transgenically rescued *Insr*$^{-/-}$ mice into *Ldlr*$^{-/-}$ mice. While animals receiving Insr-deficient BM did not display significant changes in early fatty streak lesions, they developed larger, more complex lesions at a later time-point, associated with a pronounced increase in apoptotic cells and necrotic core formation. Mechanistic studies reveal that *Insr*$^{-/-}$ macrophages

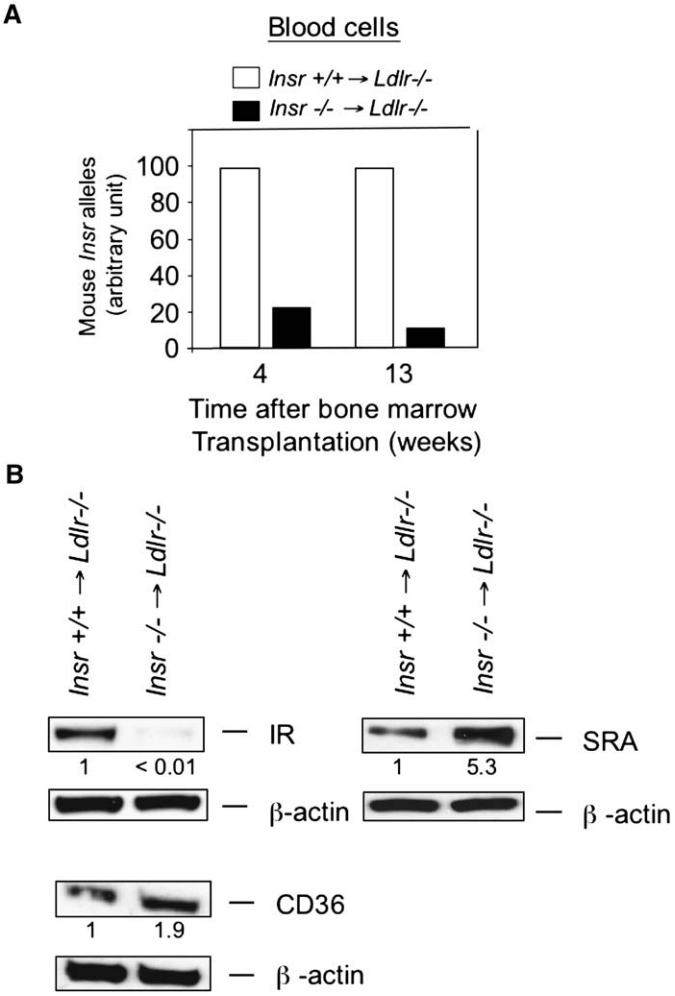

Figure 1. Characterization of blood cells and macrophages from $Ldlr^{-/-}$ mice transplanted with $Insr^{+/+}$ ($Insr^{+/+}$ → $Ldlr^{-/-}$) or $Insr^{-/-}$ ($Insr^{-/-}$ → $Ldlr^{-/-}$) bone marrow

A) The amount of mouse Insr alleles in blood cells from recipient $Ldlr^{-/-}$ mice (n = 2-3 for each genotype) at 4 or 13 weeks after bone marrow transplantation was determined by real-time quantitative PCR.

B) Protein expression of IR (insulin receptor β-subunit), SRA, CD36 in peritoneal macrophages from recipient mice (n = 3 for each genotype) after 12 weeks on the Western-type diet. Pooled macrophages were collected and cytosolic extracts were prepared. Western analysis was performed using antibodies against the proteins as indicated.

All data are representative of at least two independent experiments.

have exaggerated ER stress-mediated apoptosis, in part related to a failure to induce Akt activity during ER stress. This predisposes them to apoptosis in response to a variety of different stimuli, including those that likely play a role in late lesional macrophage death, such as free cholesterol loading.

Results

Insulin and scavenger receptor expression in transplanted mice

In order to evaluate the impact of decreased macrophage insulin signaling on atherogenesis, bone marrow was transplanted from $Insr^{-/-}$ mice into irradiated $Ldlr^{-/-}$ mice all in the C57BL6 background. Evaluation of the mouse *Insr* gene in blood cells by real-time quantitative PCR revealed an 80% reduction in $Insr^{+/+}$ alleles 4 weeks after transplantation, and a 90% reduction after 13 weeks, indicating substantial repopulation of bone marrow-derived cells by donor tissue (Figure 1A). To induce atherogenesis, animals were placed on the Western diet 5 weeks after transplantation and kept on this diet for an additional 8 or 12 weeks. Western analysis of peritoneal macrophages after 12 weeks on the diet revealed >99% reduction in Insr protein levels (Figure 1B). There was a marked (>5-fold) increase in macrophage SRA protein levels and a moderate (1.9-fold) increase in CD36 protein levels (Figure 1B). These findings are consistent with earlier studies in which we showed a posttranscriptional increase in SRA and CD36 and increased uptake of acetylated or oxidized LDL in macrophages from transgenically rescued $Insr^{-/-}$ mice (Liang et al., 2004).

Table 1. Metabolic characteristics of $Ldlr^{-/-}$ mice transplanted with $Insr^{+/+}$ or $Insr^{-/-}$ bone marrows after 12 week feeding with the Western-type diet

Donor		0 Week Western Diet	12 Week Western Diet
$Insr^{+/+}$ (N = 31)	Body weight, g	23.7 ± 0.4	25.4 ± 0.8
	Glucose, mg/dl	137.2 ± 8.1	203.6 ± 13.3
	Insulin, pg/ml	926.5 ± 70.6	1496.9 ± 104.7
	Total Cholesterol, mg/dl	220.3 ± 9.7	722.7 ± 24.1
	HDL-C, mg/dl	72.4 ± 3.7	80.9 ± 5.0
	Triglycerides, mg/dl	80.5 ± 5.2	269.4 ± 16.4
$Insr^{-/-}$ (N = 33)	Body weight, g	23.3 ± 0.3	26.7 ± 0.9
	Glucose, mg/dl	133.4 ± 7.8	193.9 ± 10.3
	Insulin, pg/ml	920.3 ± 70.3	1581.1 ± 90.9
	Total Cholesterol, mg/dl	208.5 ± 10.5	772.8 ± 20.6
	HDL-C, mg/dl	72.2 ± 2.8	92.6 ± 5.8
	Triglycerides, mg/dl	74.7 ± 5.2	328.1 ± 269.4

No significant difference in body weight and plasma parameters was found between two groups of mice fed for 12 weeks (wk).

$Insr^{-/-}$ bone marrow recipients develop larger, more complex lesions

In order to evaluate effects on atherogenesis, $Ldlr^{-/-}$ mice were placed on a high-fat, high-cholesterol (21% milk fat and 0.15% cholesterol) diet 5 weeks after the bone marrow transplantation, then maintained on this diet for either 8 or 12 weeks. Although feeding the Western diet led to mild hyperlipidemia and increased glucose and insulin levels, there was no difference in body weight, insulin, glucose, or plasma lipoprotein levels in animals receiving $Insr^{+/+}$ versus $Insr^{-/-}$ BM (Table 1). After 8 weeks on the Western diet, the animals developed typical fatty streak lesions, characterized by macrophage foam cell infiltration. However, there was no difference in lesion area (Figure 2A) or morphology (data not shown) between animals receiving $Insr^{+/+}$ versus $Insr^{-/-}$ macrophages. As assessed by Tunel and Caspase-3 staining, these early lesions contained only small numbers of apoptotic cells, and there was no difference between the groups (data not shown).

After 12 weeks on the Western diet, the $Insr^{-/-}$ BM recipients displayed lesions that were larger and strikingly more complex with increased regions of necrotic core, compared to $Insr^{+/+}$ BM recipients (arrows in Figure 2B). Quantification of lesion area revealed moderate increases in both sexes (Figure 2C). Necrotic core area was substantially increased, especially in males (Figure 2D). Necrotic cores in atherosclerotic lesions arise from macrophages that have undergone either necrotic or apoptotic

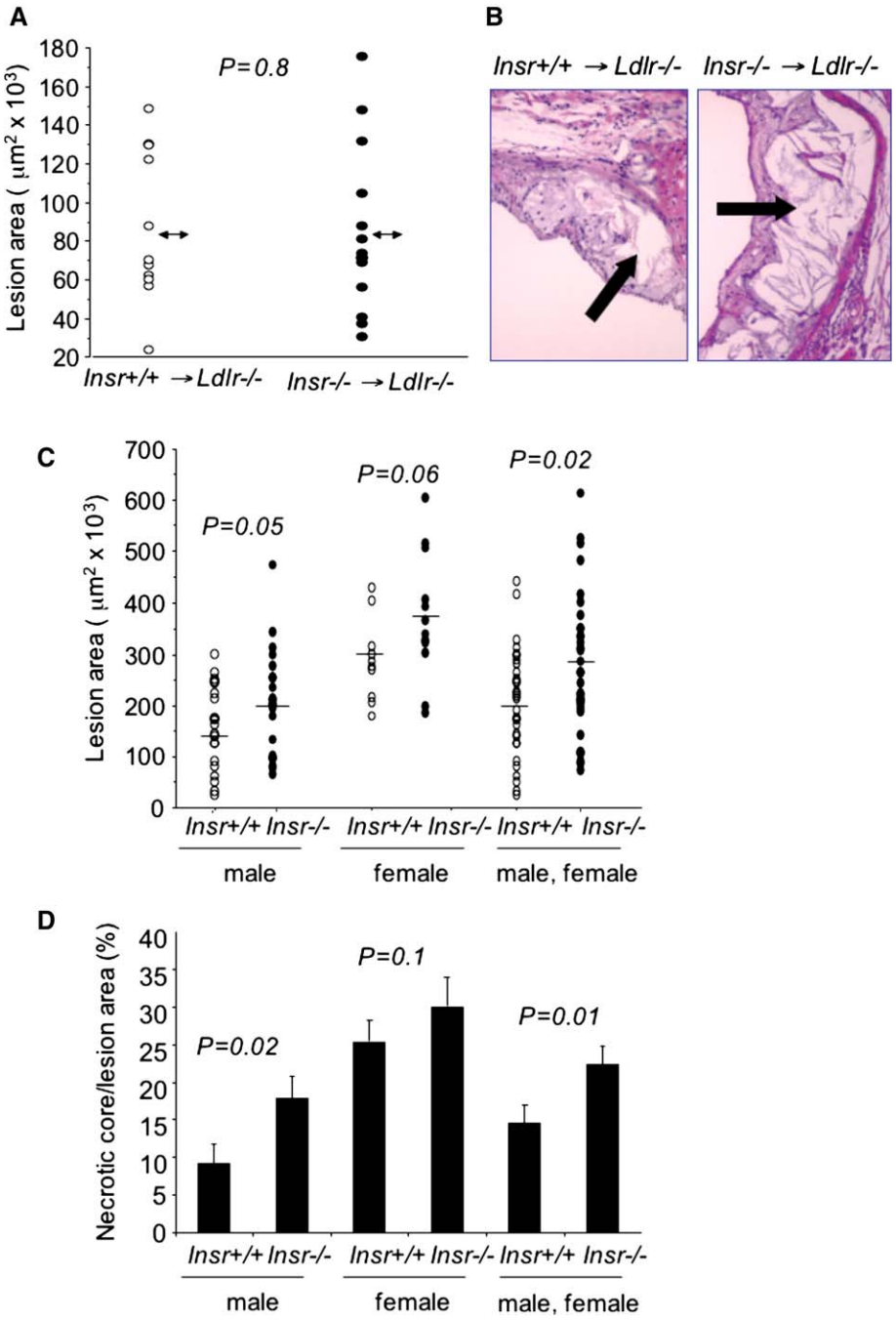

Figure 2. Atherosclerotic lesion and lipid-rich necrotic core size in proximal aortas from $Insr^{-/-}$ versus $Insr^{+/+}$ recipient $Ldlr^{-/-}$ mice

A) Atherosclerotic lesion size in proximal aortas from $Insr^{-/-}$ (n = 14) versus $Insr^{+/+}$ (n = 11) recipient *Ldlr−/−* mice fed the Western diet for 8 weeks.

B) Hematoxvlin and eosin (H&E)-stained proximal aortas from $Ldlr^{-/-}$ mice transplanted with $Insr^{+/+}$ ($Insr^{+/+}$ → $Ldlr^{-/-}$, n = 31) or $Insr^{-/-}$ ($Insr^{-/-}$ → $Ldlr^{-/-}$, n = 33) bone marrow after feeding the Western diet for 12 weeks. Arrow indicates necrotic core.

C) Quantitative analysis of H&E-stained atherosclerotic lesion area from mice in (B). Results are expressed as a scatter plot. $Insr^{+/+}$ and $Insr^{-/-}$ indicate the bone marrow genotype in $Ldlr^{-/-}$ recipient mice.

D) Quantification of necrotic core size relative to total lesion area in proximal aortas from mice in (**B**). Results are expressed as a scatter plot. $Insr^{+/+}$ and $Insr^{-/-}$ indicate the bone marrow genotype in $Ldlr^{-/-}$ recipient mice.

cell death (Ball et al., 1995). Caspase-3 and Tunel assays revealed about 2-fold increase in the number of apoptotic cells (Figure 3A and 3B). Tunel-positive regions also stained positively for Mac-3, suggesting the presence of apoptotic macrophages (data not shown). Quantification of lesion cellularity showed that macrophages were the predominant cell type, with approximately 50% of lesion area staining positive for Mac-3 in both groups of mice (data not shown). Smooth muscle cells (α-actin positive) represented approximately 12% of lesion area in both $Insr^{+/+}$ and $Insr^{-/-}$ BM recipients (data not shown). These data suggest that macrophage foam cell accumulation and initial lesion formation is similar in $Insr^{+/+}$ and $Insr^{-/-}$ BM recipients but that as lesions progress, $Insr^{-/-}$ macrophages show increased apoptosis, giving rise to more complex lesions with increased necrotic core regions.

$Insr^{-/-}$ macrophages are more susceptible to apoptosis

In view of the in vivo findings, we next determined whether $Insr^{-/-}$ macrophages were more susceptible to apoptosis in cell culture. Two different pathways relevant to macrophage apoptosis in atherosclerosis have been described, one involving the uptake of oxidized cholesterol in LDL (LDLox) and another initiated by loading with lipoprotein free cholesterol (FC). $Insr^{-/-}$ macrophages showed increased susceptibility to apoptosis induced by loading with oxidized LDL (Figure 4A). To induce free cholesterol loading, macrophages were incubated

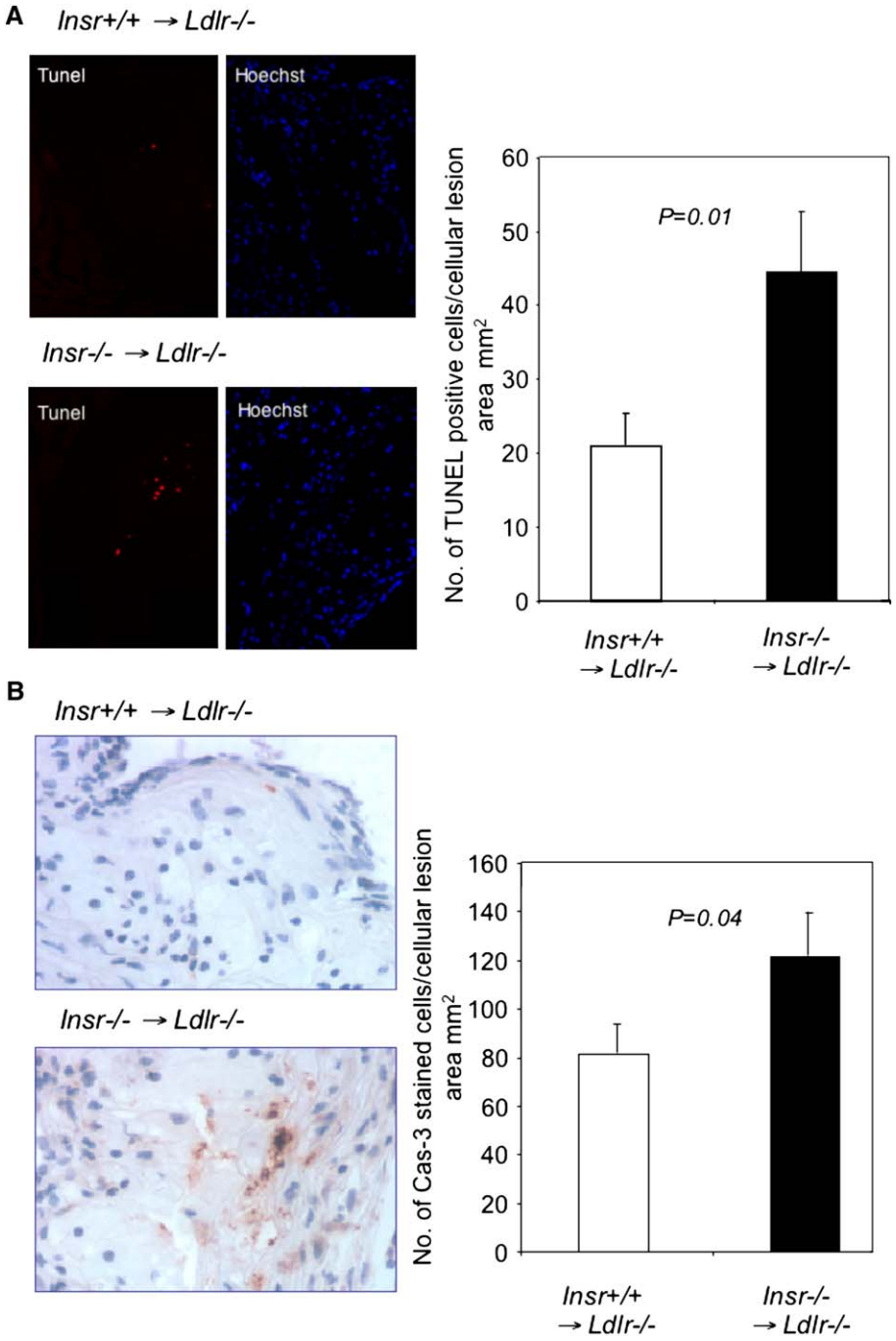

Figure 3. Increased apoptotic cell death in lesions of $Insr^{-/-}$ transplanted mice

A) Lesional apoptotic cells from $Insr^{+/+} \rightarrow Ldlr^{-/-}$ (n = 18) and $Insr^{-/-} \rightarrow Ldlr^{-/-}$ (n = 23) after 12 weeks of Western diet were detected by TUNEL staining. Representative fluorescent images (20× magnification) and quantitative data are shown. Red, Tunel-positive cell; blue, Hoechst. The data are expressed as the number of Tunel-positive cells per mm^2 cellular lesion area.

B) Lesional apoptotic cells from $Insr^{+/+} \rightarrow Ldlr^{-/-}$ (n = 24) and $Insr^{-/-} \rightarrow Ldlr^{-/-}$ (n = 27) after 12 weeks of Western diet were detected by caspase-3 staining. Representative images are shown (20× magnification). Brown staining indicates caspase-3-positive cells, and blue staining indicates hematoxylin. The data are expressed as the number of caspase-positive cells per mm^2 cellular lesion area.

with acLDL in the presence of an ACAT inhibitor, 58035. $Insr^{-/-}$ macrophages showed an approximate 2-fold increase in susceptibility to FC-induced apoptosis (Figure 4A).

Recently, Devries-Seimon et al. (2005) have shown that FC-induced apoptosis in macrophages requires a ''multihit'' mechanism involving both FC loading and ligation of SRA. While FC loading produces a UPR response, another hit involving ligation of SRA is required to produce apoptosis. $Insr^{-/-}$ macrophages show a marked increase in SRA protein levels (Figure 1B). While this is known to increase uptake of modified lipoproteins (Liang et al., 2004), we wished to determine if it also increased susceptibility to apoptosis independent of lipoprotein uptake. Thus, macrophages were loaded with FC by incubation with cyclodextrin-cholesterol (delivering cholesterol independently of the SRA) and/or treated with fucoidan (an SRA ligand) or the two treatments together (Devries-Seimon et al., 2005). In wild-type macrophages, both treatments were required to produce increased apoptosis, as reported, which was completely dependent on SRA (Devries-Seimon et al., 2005). In $Insr^{-/-}$ macrophages, the pattern of response was similar, but the magnitude of the response to SRA ligand was dramatically increased in FC-loaded cells (Figure 4B). Thus, the increase in SRA in $Insr^{-/-}$ macrophages predisposes to apoptosis both by increased uptake of modified lipoproteins and by providing

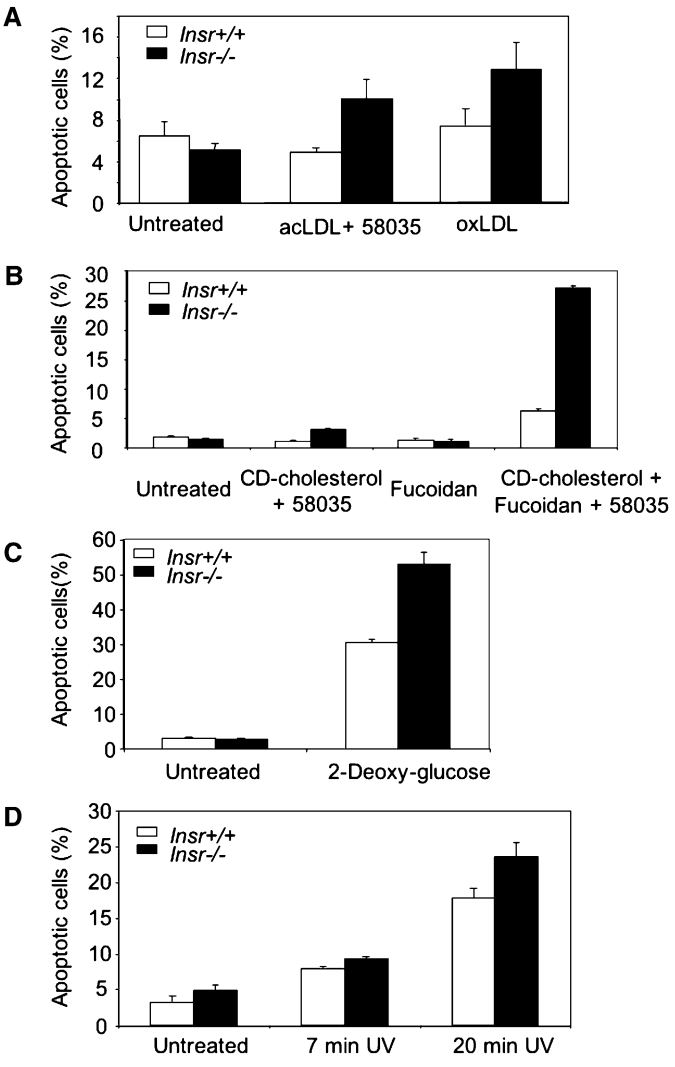

Figure 4. Increased susceptibility of *Insr*-deficient macrophages to apoptosis induced by cholesterol overload or glucose deprivation

A) Percentage of macrophages stained positive for annexin V. Pooled thioglycollate-elicited peritoneal macrophages from either $Insr^{-/-}$ or littermate ($Insr^{+/+}$) mice fed regular chow diet were incubated with or without AcLDL (100 μg/ml) and compound 58035 (10 μg/ml) or oxLDL (100 μg/ml) at 37°C for about 24 hr. Apoptosis of macrophages was determined by annexin V staining. All results represent average ± S.E. (n = 4). The relative lack of apoptosis with acLDL+ 58035 in $Insr^{+/+}$ macrophages is typically seen in thioglycollate-elicited macrophages.

B) Quantitative determination of apoptotic macrophages stained positive for annexin V. Concanavalin A-elicited peritoneal macrophages from either $Insr^{-/-}$ or littermates ($Insr^{+/+}$) mice fed regular chow diet were incubated with or without fucoidan (an SRA ligand; 25 μg/ml), cyclodextrin (CD)-cholesterol and compound 58035 (10 μg/ml), or fucoidan, CD-cholesterol, and 58035 combined at 37°C for 48 hr. Apoptosis of macrophages was determined by annexin V staining. All results represent mean ± SE (n = 4). While CD-cholesterol + fucoidan + 58035 often gives a more robust apoptotic response in wild-type macrophages than shown in this particular experiment, the marked increase seen with Insr deficiency was always observed.

C) Quantification of macrophage apoptosis induced by glucose deprivation. Pooled thioglycollate-elicited peritoneal macrophages from either $Insr^{-/-}$ or control ($Insr^{+/+}$) mice fed regular chow diet were incubated with or without 5 mM 2-Deoxy-glucose at 37°C for about 24 hr. Apoptosis of macrophages was determined by annexin V staining. All results represent average ± SE (n = 3).

D) Quantification of macrophage apoptosis induced by UV radiation. Pooled thioglycollate-elicited peritoneal macrophages from either $Insr^{-/-}$ or control ($Insr^{+/+}$) mice fed regular chow diet were incubated at 37°C for about 2 hr followed by 0, 7, and 20 min UV radiation. Apoptotic cells were stained with annexinV. All results represent average ± SE (n = 3).

another "hit" related to SRA ligation. Because loading with FC and oxidized LDL induce apoptosis by different mechanisms (Panini and Sinensky, 2001; Tabas, 2004), these findings suggested that there might be an increased susceptibility to different apoptotic stimuli in $Insr^{-/-}$ macrophages. Indeed, $Insr^{-/-}$ macrophages were more susceptible to apoptosis induced by glucose deprivation (Figure 4C). Like FC loading, glucose deprivation induces apoptosis via activation of ER stress (Park et al., 2004). Thus, we also tested the response to UV irradiation, which causes DNA damage and induces apoptosis independent of ER stress (Liang et al., 2006). There was no significant difference in apoptotic response to UV irradiation comparing $Insr^{+/+}$ and $Insr^{-/-}$ macrophages (Figure 4D). These findings suggest that $Insr^{-/-}$ macrophages may be particularly susceptible to apoptosis involving ER stress pathways.

Apoptotic pathways are not activated in $Insr^{-/-}$ macrophages in the basal state

Insulin signaling via the insulin receptor PI3 kinase and Akt has a number of different antiapoptotic effects (Amaravadi and Thompson, 2005; Osaki et al., 2004). When incubated in media containing 10% serum, Akt phosphorylation levels were similar in $Insr^{+/+}$ and $Insr^{-/-}$ macrophages (data not shown), probably reflecting a variety of inputs from growth factor and other receptors into Akt (Chakravarthy et al., 2000; Maeda et al., 2004). Furthermore, phosphorylation of the Akt substrate Gsk-3 was similar in freshly isolated $Insr^{+/+}$ or $Insr^{-/-}$ macrophages (data not shown). Evaluation of the levels of a variety of molecules involved in apoptosis including antiapoptotic proteins Mcl-1, Bfl-1, Bcl-2, and Bcl-x_L and proapoptotic factor Bax, and the expression of transcriptional repressor Bcl-6 that promotes macrophage cell death through transcriptional mechanisms, did not show significant differences between freshly isolated $Insr^{+/+}$ and $Insr^{-/-}$ macrophages (data not shown). Thus, the increased susceptibility to apoptosis of $Insr^{-/-}$ macrophages does not appear to be related to constitutive activation of apoptotic pathways.

Impaired Akt phosphorylation and increased ER stress in $Insr^{-/-}$ macrophages

The unfolded protein response (UPR) is an adaptive mechanism that helps cells to withstand ER stresses such as those produced by increased protein synthesis or glucose deprivation (Kadowaki et al., 2004; Park et al., 2004). While this adaptive response may facilitate recovery from stress, it can also lead to induction of apoptosis if stressful stimuli continue or if there are additional insults (Kadowaki et al., 2004; Kaneto et al., 2005). ER stress results in activation of phospho-PERK, which phosphorylates eIF2α inhibiting translation of many proteins and inducing GADD34 which in turn causes a homeostatic dephosphorylation of eIF2α (Oyadomari and Mori, 2004). FC loading induces the UPR and eventually leads to apoptosis as a result of induction of CHOP (Devries-Seimon et al., 2005; Feng et al., 2003). Akt activity is increased in response to ER stress produced by thapsigargin or tunicamycin treatments, leading to inhibition of ER stress-induced apoptosis (Hu et al., 2004). FC loading was also found to induce Akt phosphorylation in $Insr^{+/+}$ cells (Figure 5A). Interestingly, this Akt response was diminished and short-lived and was followed by more robust induction of CHOP in $Insr^{-/-}$ macrophages (Figure 5A). Total Akt levels were similar in cells of both genotype and did not vary during

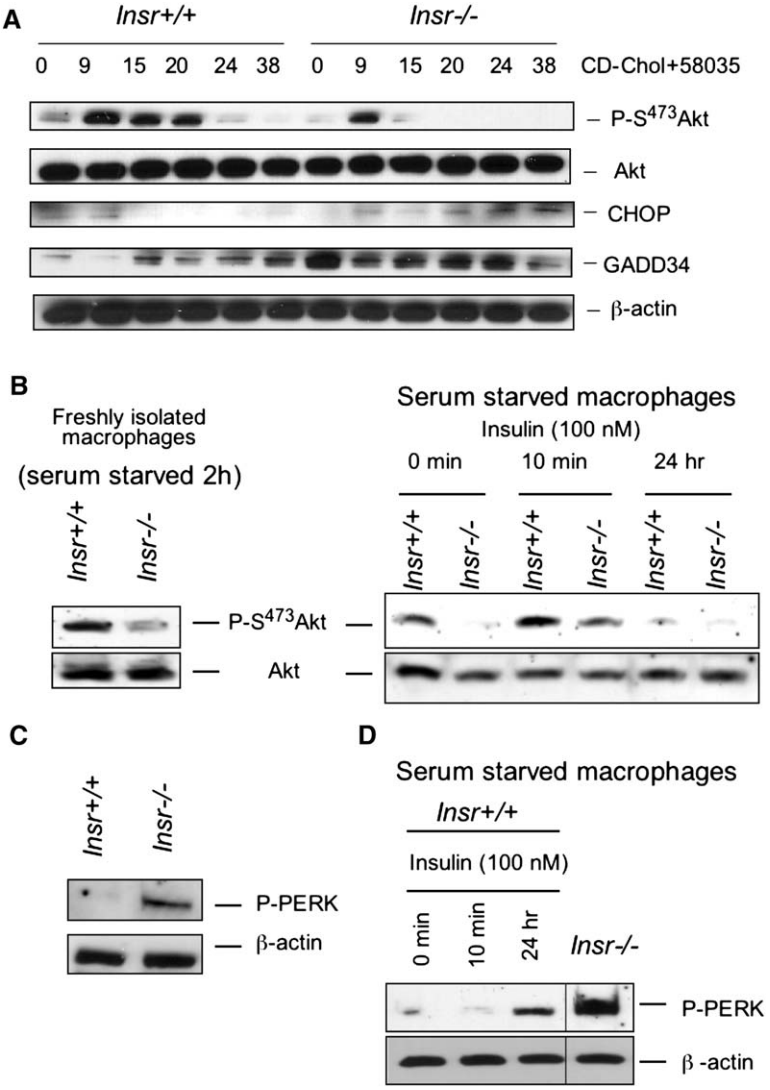

Figure 5. Impaired Akt phosphorylation and enhanced ER stress responses in $Insr^{-/-}$ macrophages during FC loading or serum deprivation

A) Decreased Akt phosphorylation and increased UPR in FC-loaded $Insr^{-/-}$ macrophages (CD cholesterol + 58035, media with serum). Concanavalin A-elicited macrophages from either $Insr^{-/-}$ or $Insr^{+/+}$ mice fed regular chow diet were treated with cyclodextrin (CD)-cholesterol and 58035 (10 μg/ml) for indicated time (hr) point in the figure. Cells were harvested and total protein extracts were prepared. Western analysis was performed with antibodies against the proteins as indicated.

B) AKT phosphorylation is reduced in $Insr^{-/-}$ macrophages. Fresh peritoneal macrophages from either $Insr^{-/-}$ or $Insr^{+/+}$ mice fed regular chow diet were treated at 37°C in DMEM with or without insulin (100 nM) for indicated time described in the figure. Cells were harvested and protein extracts were prepared. Western analysis was performed with antibodies against total Akt and P-S^{473}Akt.

C) Increased expression of an UPR marker, P-PERK, in $Insr^{-/-}$ macrophages. Fresh peritoneal macrophages from either $Insr^{-/-}$ or $Insr^{+/+}$ mice fed regular chow diet were cultured at 37°C in DMEM with 10% FBS for 2 hr. Cells were harvested and protein extracts were prepared. Western analysis was performed with antibodies against the proteins as indicated.

D) Prolonged insulin treatment caused increased P-PERK expression in $Insr^{+/+}$ macrophages. Protein expression of P-PERK in peritoneal macrophages from $Insr^{+/+}$ mice fed regular chow diet was treated at 37°C in DMEM with insulin (100 nM) for indicated time described in the figure. $Insr^{-/-}$ macrophages were cultures at 37°C in DMEM for 24h without insulin. Pooled macrophages were collected and protein extracts were prepared. Western analysis was performed using antibodies against the proteins as indicated.

the experiment. The levels of FC loading were found to be identical in $Insr^{+/+}$ and $Insr^{-/-}$ cells in response to treatment with CD-cholesterol, ruling out increased FC loading as possible explanation for the increased ER stress response in $Insr^{-/-}$ macrophages (data not shown). $Insr^{-/-}$ macrophages also showed increased levels of GADD34 at all time-points (Figure 5A) suggesting activation of the UPR even prior to FC loading. However, the additional stress of FC loading and a blunted Akt response are associated with enhanced CHOP induction and apoptosis in $Insr^{-/-}$ macrophages.

Akt phosphorylation was also markedly reduced in $Insr^{-/-}$ macrophages in response to serum starvation (Figure 5B), and this occurred in association with an enhanced UPR, as shown by induction of phospho-PERK (Figure 5C) and GADD34 (data not shown). Downregulation of insulin receptors by chronic (24 hr) high-dose insulin treatment, a commonly employed approach to mimic in vivo insulin resistance, also led to reduced Akt phosphorylation and an increased UPR response to serum starvation, albeit not to the same level as seen in $Insr^{-/-}$ cells (Figure 5B and 5D). Short-term (10 min) high-dose insulin treatment led to an increase in Akt phosphorylation, probably reflecting signaling through IGF receptors, and did not lead to phospho-PERK induction (Figures 5B and 5D). These results suggest that IR deficiency leads to an impaired ability of macrophages to induce Akt activity and to withstand stressful stimuli such as FC loading or serum starvation.

While it is evident that reduced insulin signaling could account for decreased Akt phosphorylation and activity in $Insr^{-/-}$ macrophages, it is not completely clear why Akt phosphorylation should be reduced even under basal conditions. TRB3 has been identified as an Akt associated factor that inhibits phosphorylation of Akt (Du et al., 2003). We found that TRB3 mRNA was induced more than 3.6-fold in $Insr^{-/-}$ macrophages cultured in DMEM with 10% FBS (data not shown), although TRB3 is induced as a result of ER stress through CHOP-mediated transcription (Ohoka et al., 2005). TRB3 was increased in $Insr^{-/-}$ macrophages in the absence of CHOP induction. Higher levels of TRB3 could thus be a factor explaining the lower levels of Akt phosphorylation in $Insr^{-/-}$ macrophages.

Macrophage ER stress causes a posttranscriptional induction of SRA

$Insr^{-/-}$ macrophages show a posttranscriptional induction of CD36 and SRA (Liang et al., 2004). While the induction of

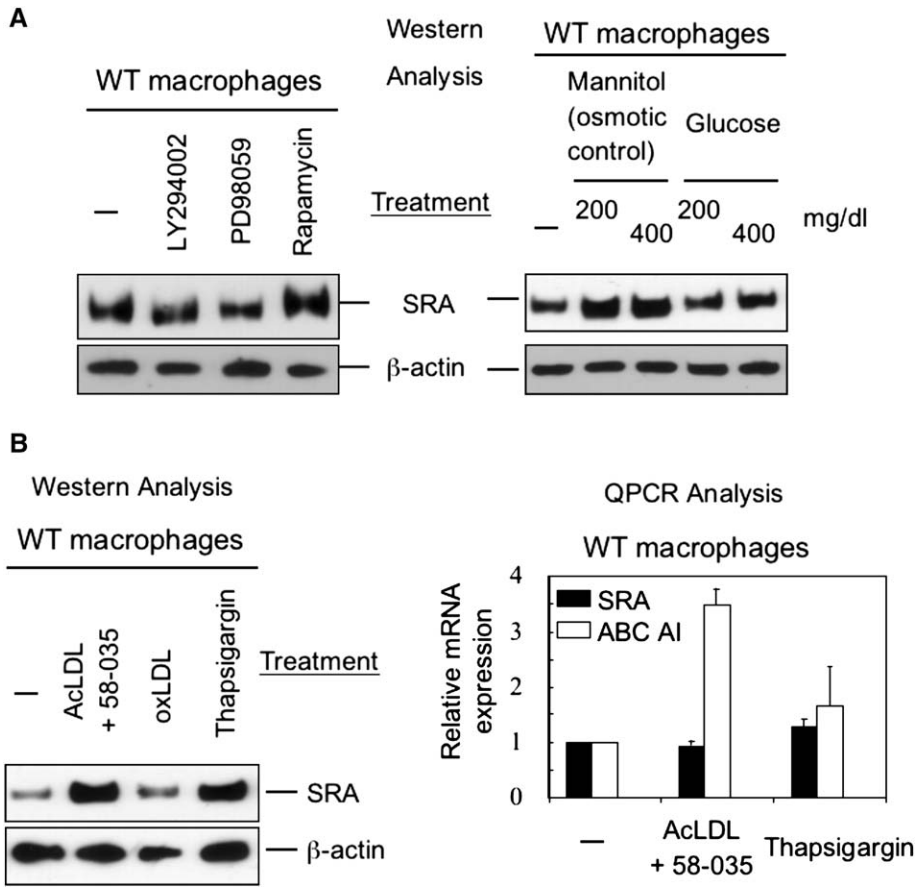

Figure 6. Macrophage ER stress response causes a posttranscriptional increase in SRA

A) Fresh peritoneal macrophages were treated at 37°C in DMEM/10% FBS with LY294002 (10 μM), PD98059 (4 μM), rapamycin (5 μM), thapsigargin (5 μM, Sigma), or corresponding vehicle controls for 24 hr, or in glucose-free DMEM/10% FBS with indicated concentrations of glucose or mannitol for 24 hr. After treatments, cell lysates were prepared for Western analysis using antibodies against SRA and β-actin.

B) Fresh peritoneal macrophages were treated at 37°C in DMEM/10% FBS with AcLDL (100 μg/ml) +58035 (10 μg/ml), oxLDL (100 μg/ml), or thapsigargin (5 μM) for 24h. After treatment, cells were harvested and total RNA or cell lysates were prepared for Western analysis and QPCR analysis. Western analysis was performed with antibodies against SRA and β-actin. The expression of SRA and ABCA1transcripts in untreated, AcLDL+58035, or thapsigargin-treated macrophages were quantified as relative mRNA expression after normalized by the expression of β-actin. Data represent average ± SE (n = 3).

CD36 could be effected by inhibition of PI3 kinase in wild-type macrophages (Liang et al., 2004), this was not the case for SRA (Figure 5A). Neither inhibition of other pathways downstream of PI3K such as mTOR nor high-glucose treatment induced SRA. Since *Insr*$^{-/-}$ macrophages show an increased ER stress response (Figure 5), we next considered the possibility that ER stress itself might lead to induction of SRA. Treatment of WT macrophages with ER stress inducers, AcLDL+58035, or thapsigargin resulted in markedly increased SRA protein with no change in SRA mRNA; as a positive control, ABCA1 mRNA was induced by FC loading (Figure 6B). Treatment with AcLDL alone had no effect on SRA levels (data not shown), indicating that the increase in SRA was a specific response to the UPR. Thus, in *Insr*$^{-/-}$ macrophages diminished Akt activity is associated with a heightened ER stress response and increased SRA expression, leading to increased apoptosis in response to SRA ligation.

Discussion

Here, we provide evidence that independent of changes in plasma lipids, insulin, or glucose levels, defective insulin signaling in bone marrow derived arterial wall cells predisposes to the formation of larger, more complex atherosclerotic plaques with increased numbers of apoptotic cells, likely representing macrophages. *Insr*-deficient macrophages showed evidence of ER stress and enhanced susceptibility to stress-induced apoptosis but not to UV-induced apoptosis. Impaired induction of Akt in response to ER stress appears to predispose *Insr*-deficient macrophages to a heightened stress response and apoptosis. ER stress causes a posttranscriptional induction of SRA, and the combination of increased ER stress and SRA ligation markedly induces apoptosis in *Insr*$^{-/-}$ macrophages (Figure 4B).

The relationship of macrophage apoptosis to atherosclerosis is complex. BM transplantation from mice deficient in AIM/SPalpha has shown that increased macrophage apoptosis is associated with decreased early lesion development (Joseph et al., 2004; Valledor et al., 2004), while BAX-deficient BM transplantation led to decreased apoptosis and increased early lesion development (Liu et al., 2005). Perhaps in early fatty streak lesions there is efficient clearance of apoptotic cells by healthy macrophages, explaining these somewhat counter-intuitive results (Tabas, 2005). Our study suggests that increased macrophage apoptosis may be associated with formation of lesions of increased complexity with larger necrotic cores. It is not clear why there was no difference in early lesion formation in our study, but perhaps there are additional defects in *Insr*-deficient macrophages that impair their phagocytic capacity. Our findings are highly consistent with recent autopsy data from human Type II diabetics who showed increased regions of necrotic core and increased macrophage apoptosis in their atherosclerotic lesions, probably predisposing to plaque rupture and sudden death (Burke et al., 2004).

A number of different factors have been implicated in apoptosis of macrophages in atherosclerotic lesions, including FC loading, growth factor withdrawal, and ATP depletion. These three factors are all known to induce ER stress and the ER stress response leads to induction of Akt activity (Hu et al., 2004). Akt

has numerous antiapoptotic effects, including direct phosphorylation and inactivation of apoptotic molecules, induction of antiapoptotic molecules as well as a variety of indirect mechanisms involving effects on cellular metabolism (Amaravadi and Thompson, 2005; Madrid et al., 2001). In addition, oxysterols associated with LDLox cause a decrease in Akt phosphorylation predisposing to macrophage apoptosis via the mitochondrial pathway (Panini and Sinensky, 2001; Salvayre et al., 2002). Finally, cross-talk between Akt and p65/NFkB may tip the balance of TNF responses in lesions toward an antiapoptotic outcome in macrophages (Kamata et al., 2005; Madrid et al., 2001).

Thus, our finding of impaired induction of Akt phosphorylation in *Insr*-deficient cells in response to ER stress likely represents a general mechanism to explain enhanced apoptotic susceptibility of macrophages with defective insulin signaling in atherosclerosis.

In addition to increased susceptibility to apoptotic stimuli, $Insr^{-/-}$ macrophages showed a heightened ER stress response. In part this could be related to the short-lived induction of Akt phosphorylation during the ER stress response (Figure 4A), perhaps related to a higher basal level of TRB3 which inhibits Akt phosphorylation (Du et al., 2003). Important targets of Akt are the FoxO transcription factors. Phosphorylation of FoxOs by Akt leads to nuclear exclusion and loss of transcriptional activity (Greer and Brunet, 2005). FoxO1 activity has been shown to lead to CHOP induction in pre-adipocytes (Nakae et al., 2003). Preliminary studies suggest decreased FoxO phosphorylation, and thus increased FoxO activity in $Insr^{-/-}$ macrophages during FC-induced ER stress (data not shown). Interestingly, an enhanced UPR has been shown to occur in the liver in association with cellular insulin resistance in ob/ob or Western diet-fed mice (Ozcan et al., 2004). The UPR can cause insulin resistance as a result of JNK-mediated serine phosphorylation of IRS-1 (Ozcan et al., 2004). Our findings suggest the converse can also be true, that decreased insulin signaling via Insr can result in induction of the UPR. This raises the possibility that in insulin-resistant stressed cells a vicious cycle could be established whereby decreased insulin signaling induces the UPR, which in turn further decreases insulin signaling.

We previously observed a posttranscriptional increase in SRA and CD36 in $Insr^{-/-}$ macrophages (Liang et al., 2004). While the induction of CD36 was related to decreased PI3 kinase activity, this was not the case for SRA. Unexpectedly, the induction of SRA was found to be a general response to the UPR, as it was induced by thapsigargin, tunicamycin and FC loading. Thus, the heightened ER stress response leads to an increase in SRA in $Insr^{-/-}$ macrophages. This increase in SRA is likely to be a major factor in the increased susceptibility of $Insr^{-/-}$ macrophages to apoptosis induced by modified lipoproteins, since it will lead both to an increase in the uptake of FC or oxysterols associated with these particles, and will provide a stronger ''second hit'' in response to SRA ligation. This suggests a new model for increased macrophage apoptosis in diabetes and metabolic syndrome that is initiated by decreased insulin signaling and is amplified by hyperlipidemia. In this model decreased insulin signaling causes an exaggerated UPR in stressed cells, leading to a posttranscriptional upregulation of the SRA. This leads to increased uptake of modified lipoproteins, further cholesterol loading, and tips the balance of the UPR toward CHOP induction and apoptosis. The diminished Akt activity in IR-deficient cells could also combine with that produced by oxysterols (Panini and Sinensky, 2001) resulting in an enhanced apoptotic response to oxidized LDL.

Experimental procedures

Animals

Transgenically rescued $Insr^{-/-}$ mice, $Insr^{-/-}$*:TTR-hInsr* mice of mixed C57BL/6J, FVB, and 129/Sv genetic backgrounds, called line L1 (Accili and Arden, 2004; Okamoto et al., 2004), were backcrossed into C57BL/6J mice. In order to estimate the extent of C57BL/6J genetic background, 90 microsatellite markers (synthesized by Invitrogen) were used for genotyping the mice in N6 generation by PCR. A range of 92%–98% of C57BL/6J background was confirmed. After one more backcross using the male donor having the highest genetic background (98%) of C57BL/6J, the N7 generation descendents were obtained and used for the experiments performed in the current study. The presence or absence of the wild-type mouse *Insr* allele and human *Insr* transgene (TTR-hInsr) was checked by PCR amplification of total genomic DNA extracted from tail biopsies (Okamoto et al., 2004). $Ldlr^{-/-}$ mice on a C57BL/6J background were purchased from The Jackson Laboratory (stock number 002207). All animal procedures used in this study followed Columbia University's institutional guidelines.

Bone marrow transplantation

Recipient $Ldlr^{-/-}$ mice were given acidified water (pH 4.5) containing 100 mg/liter neomycin (Sigma) and 10 mg/liter polymyxin B sulfate (Sigma) 1 week before and 2 weeks after BM transplantation. Eight-week-old male or female $Ldlr^{-/-}$ mice were lethally irradiated with 1000 rads (10 Gy) from a cesium g source 4 hr before transplantation. Bone marrow was collected from femurs and tibias of donor $Insr^{+/+}$ or $Insr^{-/-}$ mice by flushing with sterile medium (RPMI 1640, 2% FBS, 5 U/ml heparin, 50 U/ml penicillin, 50 μg/ml streptomycin). Each recipient mouse was injected with about 4–5 × 10^6 bone marrow cells through the tail vein. Four weeks after BM transplantation, peripheral blood was collected from the tail vein for real-time quantitative PCR to check donor bone marrow reconstitution. For the atherosclerosis study, the mice were fed the Western type diet (TD88137; Harlan Teklad) for either 8 weeks or 12 weeks beginning 5 weeks after BM transplantation.

Plasma cholesterol, triglyceride, glucose, and insulin measurements

Mice were fasted for 5–6 hr before blood samples were collected by retro-orbital venous plexus puncture. Plasma was separated by centrifugation and stored at −70ºC. HDL-C was isolated by chemical precipitation (Wako) according to manufacturer's protocol. The total plasma cholesterol, HDL-C and triglyceride were enzymatically measured using Wako enzymatic kits as previously described (Welch et al., 2001). Glucose and insulin were measured with Trinder (Sigma) and ELISA kit (Crystal Chem Inc), respectively.

Atherosclerotic lesion analysis

After either 8 weeks or 12 weeks on the Western diet, mice were anesthetized using Forane (Baxter) and killed by cervical dislocation. Mouse hearts were first perfused using 10 ml of PBS (Invitrogen), and the aortic roots were dissected and fixed in 10% formalin (Fisher). The proximal aortas were serially paraffin-sectioned and stained with hematoxvlin and eosin (Sigma) for quantification of the lesion areas using image analysis software ImagePro 3.0 Plus (Media Cybernetics). Aortic lesion size of each animal was obtained by averaging lesion areas in five sections from the same mouse. Necrotic core region was determined as acellular area of the lesions. Area was determined as the acellular area, lacking nuclei and cytoplasm, from H&E-stained sections. Necrotic core area was differentiated from regions of dense fibrous scars by the presence of macrophage debris.

In situ TUNEL assays

Apoptotic cells in atherosclerotic lesions were detected by the TUNEL (TdT-mediated dUTP nick end labeling) technique using the in situ cell death detection kit, TMR red (Roche). Sections of proximal aorta were deparaffinized, washed with buffer (PBS containing 0.2% Tween-20), incubated in 0.3% H_2O_2 for 10 min, and rinsed. For the TdT reaction, the sections were incubated in TdT reaction mixture containing TMR red dUTP for 2 hr at 37°C in a humidified chamber. After washing, genomic DNA was stained with Hoechst dye for 1 min at room temperature and then the slides were mounted with coverslips. TUNEL staining was analyzed under an Axiovert 200

fluorescence microscope (Zeiss). Fluorescent images were captured with a CCD camera and analyzed using image analysis software Photoshop (Adobe).

Immunohistochemistry

After deparaffinization, the sections on slides from proximal aortas were antigen retrieved using 1 mM EDTA, treated in 3% of H_2O_2 for 10 min to inactivate endogenous peroxidase, washed in PBS, and blocked with 10% normal goat serum (Vector Laboratories) for 1 hr at room temperature. Sections were stained with anti-rabbit caspase-3 (Cell Signaling) and biotinylated anti-rabbit antibody, incubated with horseradish peroxidase-avidin conjugate for 30 min using ABC kit (Vector Laboratories), developed with substrate diaminobenzidine, and then counterstained with hematoxylin. The immunostained sections were examined under a microscope.

Macrophage apoptosis assays

Peritoneal macrophages from transgenically rescued *Insr*$^{-/-}$ mice and wild-type control mice (n = 4 for each genotype) fed regular chow diet were harvested with PBS 3 days after intraperitoneal injection of concanavalin A (Sigma). The pooled macrophages from each strain were maintained in culture medium (DMEM supplemented with 10% FBS and 20% L-cell conditioned medium) until the cells were confluent (Feng et al., 2003). For free cholesterol loading, macrophages were then incubated with culture medium alone, medium containing SRA ligand fucoidan (25 μg/ml) (Sigma), medium containing 5 mM methyl-β-cyclodextrin (CD) (Sigma): cholesterol (5:1 mass ratio), and compound 58035 (10μg/ml), an ACAT inhibitor (Yao and Tabas, 2001), or all reagents combined for the indicated times in figure legends. Apoptosis assays were performed by staining macrophages with Alexa 488-labeled annexin V and propidium iodide (PI), using Vybrant Apoptosis Assay kit (Molecular Probes). Cells were visualized using a fluorescent microscope (Olympus, 20× magnification) equipped with CCD camera (RS Photometrics). At least three separate fields for each treatment condition were randomly selected and counted for cells positively stained for annexin V conjugate. Total cells within the field were also counted to give the percentage of cells undergoing apoptosis. For modified LDL loading, thioglycollate-elicited peritoneal macrophages maintained in DMEM with 10% FBS were incubated with AcLDL (100 μg/ml; Biomedical Technologies Inc.) and 58035 (10 μg/ml) or with oxLDL (100 μg/ml; Biomedical Technologies Inc.) for about 24 hr. Apoptosis assays were then performed as described above. For the macrophages apoptosis-induced by glucose deprivation, thioglycollate-elicited peritoneal macrophages maintained in DMEM with 10% FBS were incubated with 5mM 2-Deoxy-glucose (Sigma-Aldrich) for about 24 hr followed by the apoptosis assay described above. For the macrophages apoptosis-induced by UV radiation thioglycollate-elicited peritoneal macrophages maintained in DMEM with 10% FBS were incubated for 2 hr after the cells were UV irradiated for 0, 7, and 20 min under the UV lamp (Upland).

Ex vivo treatments of macrophages

Fresh peritoneal macrophages were treated at 37°C in DMEM/10% FBS with insulin (1 nM, Sigma), LY294002 (10 μM, Biomol), PD98059 (4 μM, Calbiochem), rapamycin (5 μM, Calbiochem), thapsigargin (5 μM, Sigma), or corresponding vehicle controls for 1 day, unless otherwise specified, or in glucose-free DMEM/10% FBS with indicated concentrations of glucose or mannitol (Sigma) for 1 day. After treatments, total RNA or cell lysates were prepared for further analysis.

Western analysis

To examine expression of IR, SRA, and CD36 protein, cell extracts of pooled peritoneal macrophages were prepared and western analysis was performed as described in Liang et al., 2004. For other proteins reported in this study, Western analysis was carried out using following primary antibodies: anti-AKT (Cell Signaling), anti-P-AKT (Cell Signaling), anti-GADD 34 (Santa Cruz Biotechnology), anti-CHOP (Santa Cruz Biotechnology), anti-PERK (Cell Signaling) and anti-β-actin antibody (Sigma). For P-Akt, CHOP and GADD34 expression, treated and control peritoneal macrophages described above were lysed (CHAPS buffer, Pierce). Protein samples were separated by SDS-PAGE and transferred onto nitrocellulose membranes (Bio-Rad). Blots were probed separately with anti-P-AKT, CHOP, GADD34 or β-actin antibody. Following incubation with horseradish peroxidase-conjugated secondary antibodies, proteins were visualized with SuperSignal West Pico Chemiluminescent reagents (Pierce) on X-ray films.

Real time quantitative PCR

To detect mouse *Insr* gene in blood cells, blood was collected from tail vein, and total genomic DNA of cells was extracted. Mouse *Insr* alleles were quantified by real time quantitative PCR with MX4000 multiplex quantitative PCR system (Stratagene). 10 ng of genomic DNA was used in each PCR reaction with mouse specific *Insr* primers (sequences are available upon request) and SYBR Green PCR core reagents (Applied Biosystems). The expression of SRA, ABCA1, and β-actin transcripts in untreated, AcLDL+58035, or thapsigargin-treated macrophages were measured using SYBR Green PCR core reagents (Applied Biosystems). The sequences of primers used are available upon request.

Statistical analysis

Results were expressed as average ± SE (n is noted in the figure legends or figures), and statistical significance of differences was evaluated with Student's t test.

Acknowledgments

We thank Dr. Song Li for help with bone marrow transplantation technique and Dr. Becky Mercer and Jennifer R. Molina for immunochemical staining techniques. T.D.-S. was supported by American Heart Association postdoctoral training grant AHA-0425805T.

Received: March 15, 2005
Revised: December 27, 2005
Accepted: February 3, 2006
Published: April 4, 2006

References

Accili, D., and Arden, K.C. (2004). FoxOs at the crossroads of cellular metabolism, differentiation, and transformation. Cell *117*, 421–426.

Amaravadi, R., and Thompson, C.B. (2005). The survival kinases Akt and Pim as potential pharmacological targets. J. Clin. Invest. *115*, 2618–2624.

Ball, R.Y., Stowers, E.C., Burton, J.H., Cary, N.R., Skepper, J.N., and Mitchinson, M.J. (1995). Evidence that the death of macrophage foam cells contributes to the lipid core of atheroma. Atherosclerosis *114*, 45–54.

Brownlee, M. (2001). Biochemistry and molecular cell biology of diabetic complications. Nature *414*, 813–820.

Burke, A.P., Kolodgie, F.D., Zieske, A., Fowler, D.R., Weber, D.K., Varghese, P.J., Farb, A., and Virmani, R. (2004). Morphologic Findings of Coronary Atherosclerotic Plaques in Diabetics. A Postmortem Study. Arterioscler. Thromb. Vasc. Biol. *24*, 1266–1271.

Chakravarthy, M.V., Abraha, T.W., Schwartz, R.J., Fiorotto, M.L., and Booth, F.W. (2000). Insulin-like growth factor-I extends in vitro replicative life span of skeletal muscle satellite cells by enhancing G1/S cell cycle progression via the activation of phosphatidylinositol 3′-kinase/Akt signaling pathway. J. Biol. Chem. *275*, 35942–35952.

Devries-Seimon, T., Li, Y., Yao, P.M., Stone, E., Wang, Y., Davis, R.J., Flavell, R., and Tabas, I. (2005). Cholesterol-induced macrophage apoptosis requires ER stress pathways and engagement of the type A scavenger receptor. J. Cell Biol. *171*, 61–73.

Du, K., Herzig, S., Kulkarni, R.N., and Montminy, M. (2003). TRB3: a tribbles homolog that inhibits Akt/PKB activation by insulin in liver. Science *300*, 1574–1577.

Feng, B., Yao, P.M., Li, Y., Devlin, C.M., Zhang, D., Harding, H.P., Sweeney, M., Rong, J.X., Kuriakose, G., Fisher, E.A., et al. (2003). The endoplasmic reticulum is the site of cholesterol-induced cytotoxicity in macrophages. Nat. Cell Biol. *5*, 781–792.

Ginsberg, H.N. (2000). Insulin resistance and cardiovascular disease. J. Clin. Invest. *106*, 453–458.

Glass, C.K., and Witztum, J.L. (2001). Atherosclerosis the road ahead. Cell *104*, 503–516.

Greer, E.L., and Brunet, A. (2005). FOXO transcription factors at the interface between longevity and tumor suppression. Oncogene *24*, 7410–7425.

Hansson, G.K. (2005). Inflammation, atherosclerosis, and coronary artery disease. N. Engl. J. Med. *352*, 1685–1695.

Hu, P., Han, Z., Couvillon, A.D., and Exton, J.H. (2004). Critical role of endogenous Akt/IAPs and MEK1/ERK pathways in counteracting endoplasmic reticulum stress-induced cell death. J. Biol. Chem. *279*, 49420–49429.

Joseph, S.B., Bradley, M.N., Castrillo, A., Bruhn, K.W., Mak, P.A., Pei, L., Hogenesch, J., O'Connell, R.M., Cheng, G., Saez, E., et al. (2004). LXR-dependent gene expression is important for macrophage survival and the innate immune response. Cell *119*, 299–309.

Kadowaki, H., Nishitoh, H., and Ichijo, H. (2004). Survival and apoptosis signals in ER stress: the role of protein kinases. J. Chem. Neuroanat. *28*, 93–100.

Kamata, H., Honda, S., Maeda, S., Chang, L., Hirata, H., and Karin, M. (2005). Reactive oxygen species promote TNFalpha-induced death and sustained JNK activation by inhibiting MAP kinase phosphatases. Cell *120*, 649–661.

Kaneto, H., Matsuoka, T.A., Nakatani, Y., Kawamori, D., Miyatsuka, T., Matsuhisa, M., and Yamasaki, Y. (2005). Oxidative stress, ER stress, and the JNK pathway in type 2 diabetes. J. Mol. Med. *83*, 429–439.

Liang, C.P., Han, S., Okamoto, H., Carnemolla, R., Tabas, I., Accili, D., and Tall, A.R. (2004). Increased CD36 protein as a response to defective insulin signaling in macrophages. J. Clin. Invest. *113*, 764–773.

Liang, S.H., Zhang, W., McGrath, B.C., Zhang, P., and Cavener, D.R. (2006). PERK (eIF2alpha kinase) is required to activate the stress-activated MAPKs and induce the expression of immediate-early genes upon disruption of ER calcium homoeostasis. Biochem. J. *393*, 201–209.

Libby, P. (2002). Inflammation in atherosclerosis. Nature *420*, 868–874.

Liu, J., Thewke, D.P., Su, Y.R., Linton, M.F., Fazio, S., and Sinensky, M.S. (2005). Reduced macrophage apoptosis is associated with accelerated atherosclerosis in low-density lipoprotein receptor-null mice. Arterioscler. Thromb. Vasc. Biol. *25*, 174–179.

Madrid, L.V., Mayo, M.W., Reuther, J.Y., and Baldwin, A.S., Jr. (2001). Akt stimulates the transactivation potential of the RelA/p65 Subunit of NF-kappa B through utilization of the Ikappa B kinase and activation of the mitogen-activated protein kinase p38. J. Biol. Chem. *276*, 18934–18940.

Maeda, H., Rajesh, K.G., Suzuki, R., and Sasaguri, S. (2004). Epidermal growth factor and insulin inhibit cell death in pancreatic beta cells by activation of PI3-kinase/AKT signaling pathway under oxidative stress. Transplant. Proc. *36*, 1163–1165.

Moore, K.J., Kunjathoor, V.V., Koehn, S.L., Manning, J.J., Tseng, A.A., Silver, J.M., McKee, M., and Freeman, M.W. (2005). Loss of receptor-mediated lipid uptake via scavenger receptor A or CD36 pathways does not ameliorate atherosclerosis in hyperlipidemic mice. J. Clin. Invest. *115*, 2192–2201.

Nakae, J., Kitamura, T., Kitamura, Y., Biggs, W.H., 3rd, Arden, K.C., and Accili, D. (2003). The forkhead transcription factor Foxo1 regulates adipocyte differentiation. Dev. Cell *4*, 119–129.

Nathan, D.M., Lachin, J., Cleary, P., Orchard, T., Brillon, D.J., Backlund, J.Y., O'Leary, D.H., and Genuth, S. (2003). Intensive diabetes therapy and carotid intima-media thickness in type 1 diabetes mellitus. N. Engl. J. Med. *348*, 2294–2303.

Ohoka, N., Yoshii, S., Hattori, T., Onozaki, K., and Hayashi, H. (2005). TRB3, a novel ER stress-inducible gene, is induced via ATF4-CHOP pathway and is involved in cell death. EMBO J. *24*, 1243–1255.

Okamoto, H., Nakae, J., Kitamura, T., Park, B.C., Dragatsis, I., and Accili, D. (2004). Transgenic rescue of insulin receptor-deficient mice. J. Clin. Invest. *114*, 214–223.

Osaki, M., Oshimura, M., and Ito, H. (2004). PI3K-Akt pathway: its functions and alterations in human cancer. Apoptosis *9*, 667–676.

Oyadomari, S., and Mori, M. (2004). Roles of CHOP/GADD153 in endoplasmic reticulum stress. Cell Death Differ. *11*, 381–389.

Ozcan, U., Cao, Q., Yilmaz, E., Lee, A.H., Iwakoshi, N.N., Ozdelen, E., Tuncman, G., Gorgun, C., Glimcher, L.H., and Hotamisligil, G.S. (2004). Endoplasmic reticulum stress links obesity, insulin action, and type 2 diabetes. Science *306*, 457–461.

Panini, S.R., and Sinensky, M.S. (2001). Mechanisms of oxysterol-induced apoptosis. Curr. Opin. Lipidol. *12*, 529–533.

Park, H.R., Tomida, A., Sato, S., Tsukumo, Y., Yun, J., Yamori, T., Hayakawa, Y., Tsuruo, T., and Shin-ya, K. (2004). Effect on tumor cells of blocking survival response to glucose deprivation. J. Natl. Cancer Inst. *96*, 1300–1310.

Pirro, M., Mauriege, P., Tchernof, A., Cantin, B., Dagenais, G.R., Despres, J.P., and Lamarche, B. (2002). Plasma free fatty acid levels and the risk of ischemic heart disease in men: prospective results from the Quebec Cardiovascular Study. Atherosclerosis *160*, 377–384.

Reaven, G.M. (2002). Multiple CHD risk factors in type 2 diabetes: beyond hyperglycaemia. Diabetes Obes. Metab. *4* (*Suppl 1*), S13–S18.

Salvayre, R., Auge, N., Benoist, H., and Negre-Salvayre, A. (2002). Oxidized low-density lipoprotein-induced apoptosis. Biochim. Biophys. Acta *1585*, 213–221.

Steinberg, H.O., and Baron, A.D. (2002). Vascular function, insulin resistance and fatty acids. Diabetologia *45*, 623–634.

Tabas, I. (2004). Apoptosis and plaque destabilization in atherosclerosis: the role of macrophage apoptosis induced by cholesterol. Cell Death Differ. *11* (*Suppl 1*), S12–S16.

Tabas, I. (2005). Consequences and therapeutic implications of macrophage apoptosis in atherosclerosis: the importance of lesion stage and phagocytic efficiency. Arterioscler. Thromb. Vasc. Biol. *25*, 2255–2264.

Valledor, A.F., Hsu, L.C., Ogawa, S., Sawka-Verhelle, D., Karin, M., and Glass, C.K. (2004). Activation of liver X receptors and retinoid X receptors prevents bacterial-induced macrophage apoptosis. Proc. Natl. Acad. Sci. USA *101*, 17813–17818.

Vicent, D., Ilany, J., Kondo, T., Naruse, K., Fisher, S.J., Kisanuki, Y.Y., Bursell, S., Yanagisawa, M., King, G.L., and Kahn, C.R. (2003). The role of endothelial insulin signaling in the regulation of vascular tone and insulin resistance. J. Clin. Invest. *111*, 1373–1380.

Vikramadithyan, R.K., Hu, Y., Noh, H.L., Liang, C.P., Hallam, K., Tall, A.R., Ramasamy, R., and Goldberg, I.J. (2005). Human aldose reductase expression accelerates diabetic atherosclerosis in transgenic mice. J. Clin. Invest. *115*, 2434–2443.

Welch, C.L., Bretschger, S., Latib, N., Bezouevski, M., Guo, Y., Pleskac, N., Liang, C.P., Barlow, C., Dansky, H., Breslow, J.L., and Tall, A.R. (2001). Localization of atherosclerosis susceptibility loci to chromosomes 4 and 6 using the Ldlr knockout mouse model. Proc. Natl. Acad. Sci. USA *98*, 7946–7951.

Williams, K.J., and Tabas, I. (1998). The response-to-retention hypothesis of atherogenesis reinforced. Curr. Opin. Lipidol. *9*, 471–474.

Yao, P.M., and Tabas, I. (2001). Free cholesterol loading of macrophages is associated with widespread mitochondrial dysfunction and activation of the mitochondrial apoptosis pathway. J. Biol. Chem. *276*, 42468–42476.